CHAPTER

18 CHARACTERIZING THE VARIATION IN ATMOSPHERIC RADIATION AT AVIATION ALTITUDES

W. Kent Tobiska[*,†], **Matthias M. Meier**[‡], **Daniel Matthiae**[‡], **Kyle Copeland**[§]

Space Environment Technologies, Pacific Palisades, CA, United States[*] *Utah State University, Logan, UT, United States*[†] *Deutsches Zentrum für Luft- und Raumfahrt e.V. (DLR), German Aerospace Center, Institute of Aerospace Medicine, Cologne, Germany*[‡] *Federal Aviation Administration, Civil Aerospace Medical Institute, Oklahoma City, OK, United States*[§]

CHAPTER OUTLINE

1 RADIATION SOURCES AND THEIR EFFECTS ON AVIATION

The aerospace environment has several sources of ionizing radiation. Exposure to this radiation is one of the natural hazards faced by aircrew, high-altitude pilots, frequent flyers, and, eventually, commercial space travelers. Galactic cosmic rays (GCRs) and solar energetic particles (SEPs) (Fig. 1) almost always are the most important sources of ionizing radiation, particularly when traveling at or above commercial aviation altitudes (8 km or 26,000 ft; Friedberg & Copeland, 2003, 2011; Tobiska et al., 2016).

Extreme Events in Geospace. https://doi.org/10.1016/B978-0-12-812700-1.00018-2

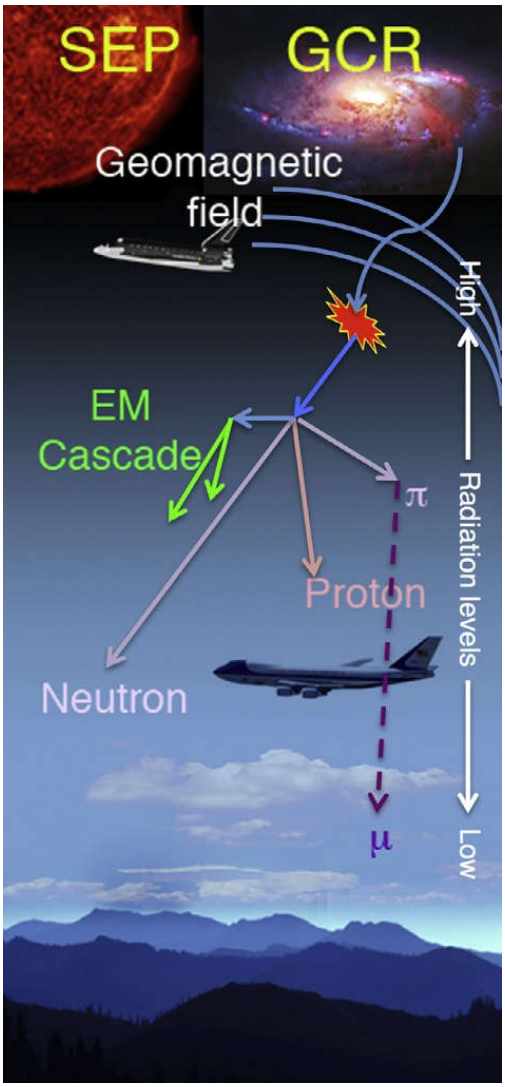

FIG. 1

Sources of primary and secondary cosmic radiation.

GCRs originate from outside the solar system and consist mostly of energetic protons (p^+), with some alpha particles (α) and a few heavier ions (HZE) such as iron (Fe^{26+}) (about 87 p^+:12 α:1 HZE from Simpson, 1983). SEPs originate on the Sun. They are similar in composition to GCRs, being predominantly protons, but with relatively fewer heavier ions. GCRs and SEPs are sometimes collectively referred to as *cosmic rays*.

Regardless of their source, some of these particles transit Earth's magnetosphere and interact with its atmosphere. Cosmic ray particle access to the neutral atmosphere depends upon rigidity (ratio of momentum to charge: particles of the same rigidity follow similar paths in a magnetic field). The Earth's magnetic field acts similar to a high-pass rigidity filter, and cosmic radiation particle access

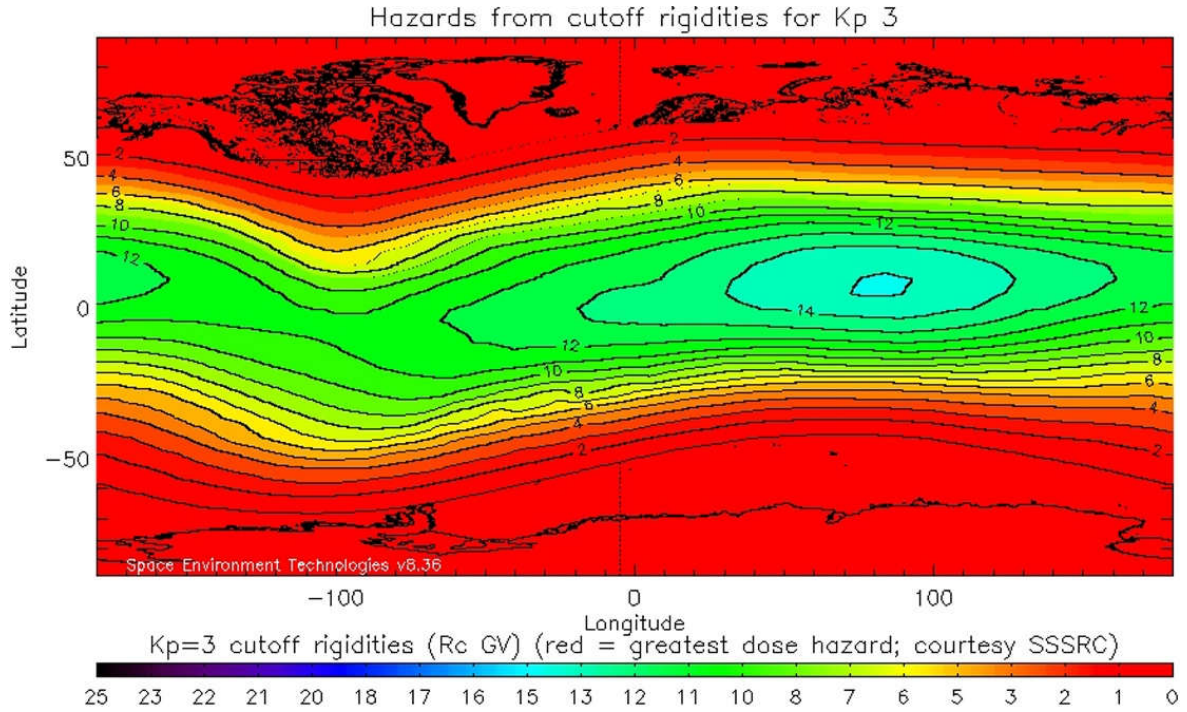

FIG. 2

Effective vertical magnetic cutoff rigidities for the 2010 epoch calculated by Smart and Shea using the IGRF 2010 internal reference field for *Kp*=3; the color bar indicates the notional hazard level based on the increased (lower rigidity) particle flux at higher latitudes (Shea & Smart, 2012).

is well described using a quantity called cutoff rigidity (Fig. 2). During normal geomagnetic conditions, cutoff rigidity varies approximately inversely with geographic latitude; only particles with relatively high rigidity can make it to the atmosphere at latitudes near the equator, while even the lowest rigidity particles can enter the atmosphere at the geomagnetic poles. As a result, the highest primary radiation fluxes enter at high latitudes, with maxima surrounding the geomagnetic poles.

Below the terrestrial atmosphere's mesopause near 85 km, the particles increasingly interact with neutral species, which are predominantly N_2 and O_2. The particle collisions with these target molecules create sprays of secondary and tertiary particles as well as photons with lower energies (collectively called *secondaries*), converting some of the initiating particle's energy into new particles (if the primary cosmic ray particle has enough energy, there will be many generations of secondary particles, called a *shower*) (Fig. 1). The secondaries in the showers produced by cosmic radiation include neutrons (n), p^+, e^-, e^+, α (and other nuclear fragments), pions (π), muons (μ), γ-rays, and x-rays (and to a much lesser degree more exotic particles). Under normal, GCR-dominated conditions (when there is no significant SEP contribution to atmospheric ionizing radiation) the primary particles lose energy, the secondary population increases, and the total ionization increases until this results in a maximum ionization rate between 15 and 20 km (49,000–65,000 ft) called the Regener-Pfotzer maximum (Regener & Pfotzer, 1935). During a time of increased SEP radiation, the relatively high flux and low average energy of the SEP particles compared to GCR can move the Regener-Pfotzer maximum to higher altitudes. Below the Regener-Pfotzer maximum down to the Earth's surface, the ionization

rate continues to decrease because particles and photons are absorbed in an increasingly thick atmosphere. All of these particles are able to collide with an aircraft hull and its interior components, people, or fuel to further alter the radiation spectrum that affects tissue and avionics (IARC, 2000; UNSCEAR, 2000).

In human tissues, radiation can activate several injury pathways by causing atoms and molecules to become ionized, dissociated, or excited. These include (i) production of free radicals, (ii) breakage of chemical bonds, (iii) production of new chemical bonds and cross-linkage between macromolecules, and (iv) damage of molecules that regulate vital cell processes, such as deoxyribonucleic acid (DNA), ribonucleic acid (RNA), and proteins (UNSCEAR, 2000). Evidence indicates that high linear energy transfer (LET, a measure of energy lost by a radiation per unit track length) radiations are generally more harmful to living tissues per unit dose (energy deposited per unit of target mass) than low-LET radiations. Low-LET radiations include photons, muons, and electrons, while high-LET radiations are particles such as neutrons, alpha particles, and heavier ions. Protons and charged pions are often also considered low-LET radiation, but interact more like high-LET radiations often enough to be treated separately in dosimetry (ICRP, 2007). Although cells can usually repair damage from low doses of ionizing radiation, particularly if it is low-LET radiation such as that received daily from ambient radiation near the surface of the Earth, cell death is the most likely result from higher doses. At extremely high doses, the cell population in an organ can drop so rapidly that cells cannot be replaced quickly enough and the tissue fails to function normally (IARC, 2000; UNSCEAR, 2000). Even the mildest effects related to this mechanism are not observed until absorbed doses exceed 100 mGy;such doses or corresponding dose rates have not been observed as a result of cosmic radiation in the atmosphere so far, only from technological sources. Such extreme levels of radiation have only been theoretically calculated for hypothetical, extreme solar particle events (Fig. 3). Epidemiological studies in occupational groups have been conducted for several decades, usually with a focus on radiation-associated cancer, and there continues to be a broad discussion in this field of study.

In addition to potential health effects including an increased lifetime risk of cancer, damage to avionics is a matter of concern because it might endanger the safety of a flight (Dyer & Truscott, 1999; Dyer & Lei, 2001; Dyer et al., 2003). While this paper does not pursue a detailed discussion related to radiation effects on avionics, interested readers in this subject matter are pointed to a wide body of work. This includes studies and reports (Normand et al., 1994, 2006; Mutuel, 2016) as well as standards such as the International Commission on Radiation Units (ICRU) Joint Report (84), the International Electrotechnical Commission (IEC) SEE standard for avionics (International Electrotechnical Commission (IEC) 62396–1, 2012), the Joint Electron Device Engineering Council Solid State Technology Association (JEDEC) SEE standard for avionics (JESD89A), the World Meteorological Organization observing requirements (#709, #738), and the International Civil Aviation Organization (ICAO) regulatory guidelines (Standards and Recommended Practices 3.8.1).

2 STATUS OF MODELS

There have been many models developed that are capable of specifying the aviation radiation environment. They represent the breadth and depth of work done in this field for many years. Recently developed models include: AIR (Johnston, 2008), AVIDOS (Latocha et al., 2009; Latocha et al.,

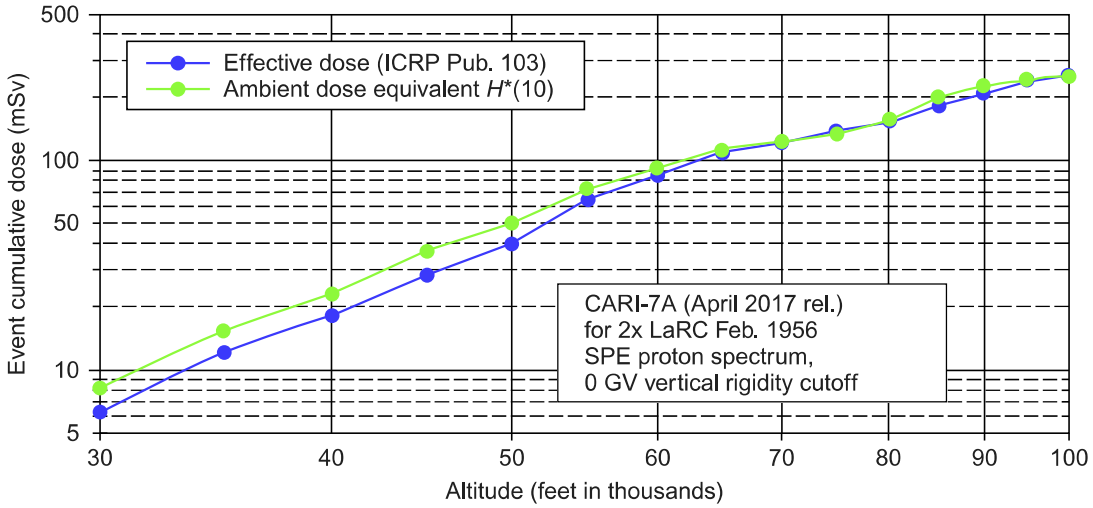

FIG. 3

Effect of altitude on the cumulative ambient equivalent $H^*(10)$ and effective doses for an extreme solar proton event at a polar location (0 GV vertical cutoff rigidity). For this example, twice the LaRC spectrum proton for the Feb. 1956 event was used, which remains the largest event to date of the neutron monitor era (Singleterry et al., 2010). CARI-7A was used for the calculations (Copeland, 2017).

2014), CARI-7 (Copeland, 2017), EPCARD.NET (Mares et al., 2009), FDOSCalc (Wissmann et al., 2010), FREE (Felsberger et al., 2009), KREAM (Hwang et al., 2014), NAIRAS (Mertens et al., 2013), PANDOCA (Matthiä et al., 2014), PARMA/EXPACS (Sato et al., 2008; Sato, 2015), and PC-AIRE (McCall et al., 2009). While all of these models are based on data, the data needed to drive an individual model varies from model to model. At one extreme are models like PC-AIRE and FDOSCalc, which are built from empirical functions fit to in-flight measurement databases. At the other extreme are models like CARI-7, EPCARD.NET, NAIRAS, and PANDOCA, which start from the particle spectrum (SEP or GCR local interstellar spectrum, based on measurements) and then model propagation of the particles through Earth's magnetosphere and atmosphere (and heliosphere for GCRs) using a collection of previously developed physics models. As an example of recent work, Joyce et al. (2014) utilized Monte Carlo simulations of showers coupled to CRaTER measurements (Spence et al., 2010; Schwadron et al., 2012) in deep space to estimate dose rates through the Earth's atmosphere at a range of different altitudes down to aviation heights. While most models could be used for nowcasting with proper data input and enough computing power, the purpose for their development was typically for retrospective evaluations.

3 STATUS OF MEASUREMENTS

Ground-based continuous monitoring of cosmic radiation-related particle data has been ongoing for more than half a century, using neutron monitors, ion chambers, muon telescopes, and other instruments. Space-based monitoring has been regularly performed since the start of the Geosynchronous Operational Environmental Satellite (GOES) program in the 1970s. But until recently, the typical method of measuring dose at commercial aviation altitudes was by in situ instruments that were

returned after flight for analysis. A wealth of data related to the aviation radiation environment has made important contributions to model validations of the radiation field at altitude, especially for dose in human tissue. The vast majority of these measurements were made with the Tissue Equivalent Proportional Counters (TEPCs) under GCR background conditions, with very few solar events captured (perhaps fortunately, large SEP events are very rare) (Dyer et al., 1990; Beck et al., 1999; Kyllönen et al., 2001; ECRP 140, 2004; Getley et al., 2005; Beck et al., 2005; Latocha et al., 2007; Meier et al., 2009, 2016a,b; Beck et al., 2009; Dyer et al., 2009; Hands & Dyer, 2009; Getley et al., 2005; Gersey et al., 2012; and Tobiska et al., 2014a,b, 2015). Some solid-state detectors have been used (Dyer et al., 2009; Hands & Dyer, 2009; Ploc et al., 2013; Lee et al., 2015; Tobiska et al., 2016).

To date, however, the difficult task of continuous radiation environment monitoring, reporting, and modeling has not yet been achieved, putting extreme event monitoring at a disadvantage. Because monitoring does not exist, and because very few in-flight radiation measurements during significant SPEs have occurred, it remains an important task to fly calibrated instruments as widely and often as possible. This is needed to enable the accumulation of a data volume that can both validate models and potentially assist in creating data-assimilated "weather" of the radiation environment, similar to what has occurred in the tropospheric weather community during the past few decades.

4 STATUS OF MONITORING FOR EXTREME CONDITIONS

The most commonly used data in evaluation of past extreme space weather events has come from neutron monitors (Carmichael, 1964; Hatton, 1971; Simpson, 2000). In particular, ground level enhancements (GLEs) from solar cosmic rays have been used to identify extreme conditions for the aviation radiation environment with respect to dose rates above the background cosmic radiation levels. Neutron monitor data have been extremely useful for evaluation of the largest SEP events (O'Brien & Sauer, 2000; Copeland et al., 2008; Al Anid et al., 2009; Meier & Matthiä, 2014). Many works have studied this topic in detail (O'Brien et al., 1996; Gerontidou et al., 2002; Iles et al., 2004; Andriopoulou et al., 2011; Shea & Smart, 2012; McCracken et al., 2012; Mishev et al., 2015; Atwell et al., 2016) and a general conclusion from this body of work is that the energy spectra of GLEs are not identical to one another. Shea (private communication, 2017) has provided a list of 71 GLEs from 1942 through May 2012. The hardness, or particle energy distribution, is a feature that most distinguishes GLEs. For example, a hard spectra event of GLE 57 (May 6, 1998) showed a neutron monitor increase of 4% in the polar regions with a maximum integral >10 MeV proton flux increase of 239 protons cm^{-2} s^{-1} sr^{-1}. However, a soft spectra solar proton event on Nov. 8, 2000, had a maximum integral >10 MeV proton flux of 14,800 protons cm^{-2} s^{-1} sr^{-1} but also had no observable increase in neutron monitor datasets (Shea & Smart, 2012). Thus, not all proton events and GLEs are the same. Because a rigorous discussion of this topic is beyond the scope of this chapter, we will illustrate spectral differences with the example of a small number of GLE cases in the following discussion.

We note that coupling radiation transport models to neutron monitor data has been highly successful for monitoring variations in GCRs associated with changes in solar activity; this capability is incorporated into many of the models mentioned above. However, neutron monitor sensitivity to SEP radiation is limited by atmospheric and geomagnetic shielding, which are both much more effective for SEP radiation. While shielding has been identified, to some extent, by careful selection of monitoring sites with placement at different altitudes and latitudes and longitudes, the instruments are very massive, and thus poorly suited for in-flight use. Only the largest events can be observed, and often only

at high latitudes. Another issue with neutron monitor use is that universities or science institutes operate many of these instruments with limited staff and budgets. These are often insufficient to support operational applications; thus, obtaining global data in near real time has been difficult or impractical. While older data are available from http://www.nmdb.eu/ and http://cr0.izmiran.ru/common/links.htm, some data providers have occasionally been reluctant to make their data available for operational users because corrections to generate the highest quality data may take a year or more to complete. These corrections account for local effects such as terrestrial weather as well as subtle changes that occur as the instruments age. Overall, the number of neutron monitor instruments supported has declined steadily for the past few decades even though there is broad interest in continuing these observations.

Continuous satellite-based monitoring of cosmic rays has augmented neutron monitor and other ground-based instrument data since the early 1970s. For aviation the most useful of these have been the particle detectors on GOES operated by the U.S. National Oceanic and Atmospheric Administration (NOAA). Unlike most satellite particle detectors, the detectors on GOES provide data for a wide energy range of protons and alpha particles from a few MeV to >1 GeV. The low-energy particles dominate the measurements and, thus, these satellites provide the SEP particle spectrum that does not generate a significant neutron monitor response because the particle energies are too low. The detectors have been limited by their upper energy threshold and directional sensitivity.

The early stages of a more practical monitoring capability are now being constructed. Among many possible models, one example of the current state of the art for an operational system is NASA Langley Research Center's (LaRC) *Nowcast of Atmospheric Ionizing Radiation for Aviation Safety* (NAIRAS) system (Mertens et al., 2012, 2013). NAIRAS is a data-driven, physics-based climatological model (Fig. 4) producing time-averaged weather conditions using the HZETRN radiation transport code that characterizes the global radiation environment from the surface to low Earth orbit (LEO) for dose rate and total dose hazards. Global, data-driven results are reported hourly at the NAIRAS public URL of http://sol.spacenvironment.net/~nairas/index.html. However, to produce the weather of the radiation environment, NAIRAS, as an example, needs assimilated real-time data. Consider the analogy of tropospheric weather models that need temperature, pressure, and humidity to make accurate weather reports. Similarly, for specifying radiation weather, models need data in near real time and from global locations. NAIRAS input data for assimilation could consist of total ionizing dose (TID), that is, absorbed dose in silicon or more complex dosimetric values where available.

The NASA *Automated Radiation Measurements for Aerospace Safety* (ARMAS) program creates these real-time TID data. For data assimilation into operational NAIRAS (Tobiska et al., 2015), TID can be used as an index (indicator of level of activity) for full energy spectrum measurements that is analogous to how total electron content (TEC) is used in ionospheric data assimilation models. ARMAS uses a TID commercial-off-the-shelf (COTS) microdosimeter combined with an Iridium data link to report the absorbed dose, $D(\mathrm{Si})$, from aircraft during flight. Between 2013 and 2017, ARMAS has obtained real-time radiation measurements from the ground to 17 km for 360 flights with 251,926 one-minute $\dot{D}(\mathrm{Si})$, $\dot{D}(\mathrm{Ti})$, $\dot{H}$, $\dot{E}$, and $\dot{H}^*(10)$ observed and derived data records (Tobiska et al., 2016). The data are available at the ARMAS URL http://sol.spacenvironment.net/armas_ops/Archive/ with an example shown in Fig. 5. The ARMAS data records are comparable in scope to the decade-long Liulin dataset (Ploc et al., 2013), which is also available online at http://hroch.ujf.cas.cz/~aircraft/ and contains 3699 flights with 133,438 $H^*(10)$ records having 5-minute resolution and covering one solar cycle from 2001 to 2011. The accuracy of all datasets continues to be assessed.

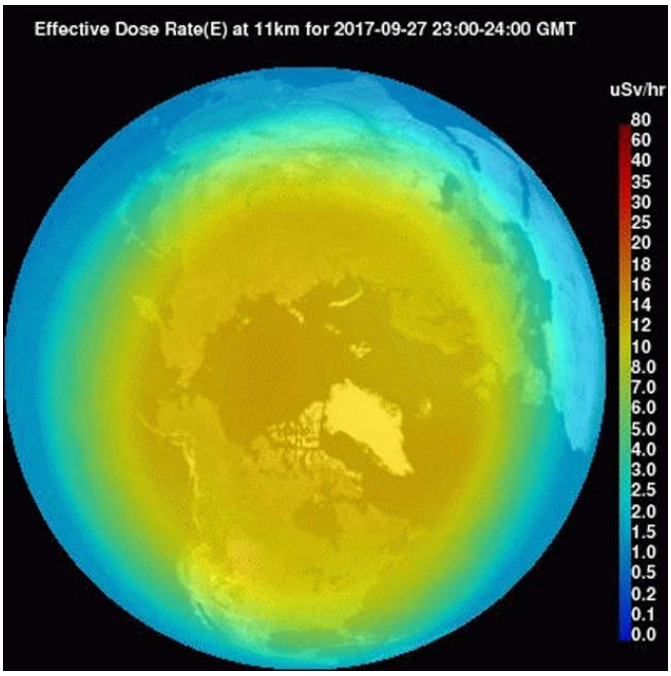

FIG. 4

Effective doses rates calculated for 11-km altitude by NAIRAS for the northern hemisphere on May 12, 2017 (Mertens et al., 2012, 2013).

A recent measurement project was the NASA Radiation Dosimetry Experiment (RaD-X) stratospheric balloon project (Mertens et al., 2016). RaD-X obtained dosimetric measurements from a balloon platform that was used to characterize cosmic ray primaries. In addition, radiation detectors were flown to assess their application to long-term, continuous monitoring of the aircraft radiation environment. The RaD-X balloon was launched from Fort Sumner, New Mexico, on Sept. 25, 2015. More than 18 h of flight data were obtained from each of the four different science instruments at altitudes above 20 km. The balloon data were supplemented by contemporaneous aircraft measurements. Flight-averaged dosimetric quantities were reported at seven altitudes to provide benchmark measurements for improving aviation radiation models. The altitude range of the flight data extends from commercial aircraft altitudes to above the Regener-Pfotzer maximum where the dosimetric quantities are influenced by cosmic ray primaries.

5 CLASSIFICATION OF AVIATION-RELEVANT EXTREME SPACE WEATHER RADIATION EVENTS

The assessment of space weather events in general and the identification of extreme space weather events in particular depend on the variation of observable physical parameters as well as upon their impacts and consequences. The challenge of quantifying space weather events related to aviation radiation, for practical purposes, consists in finding a relevant index that connects an observable physical

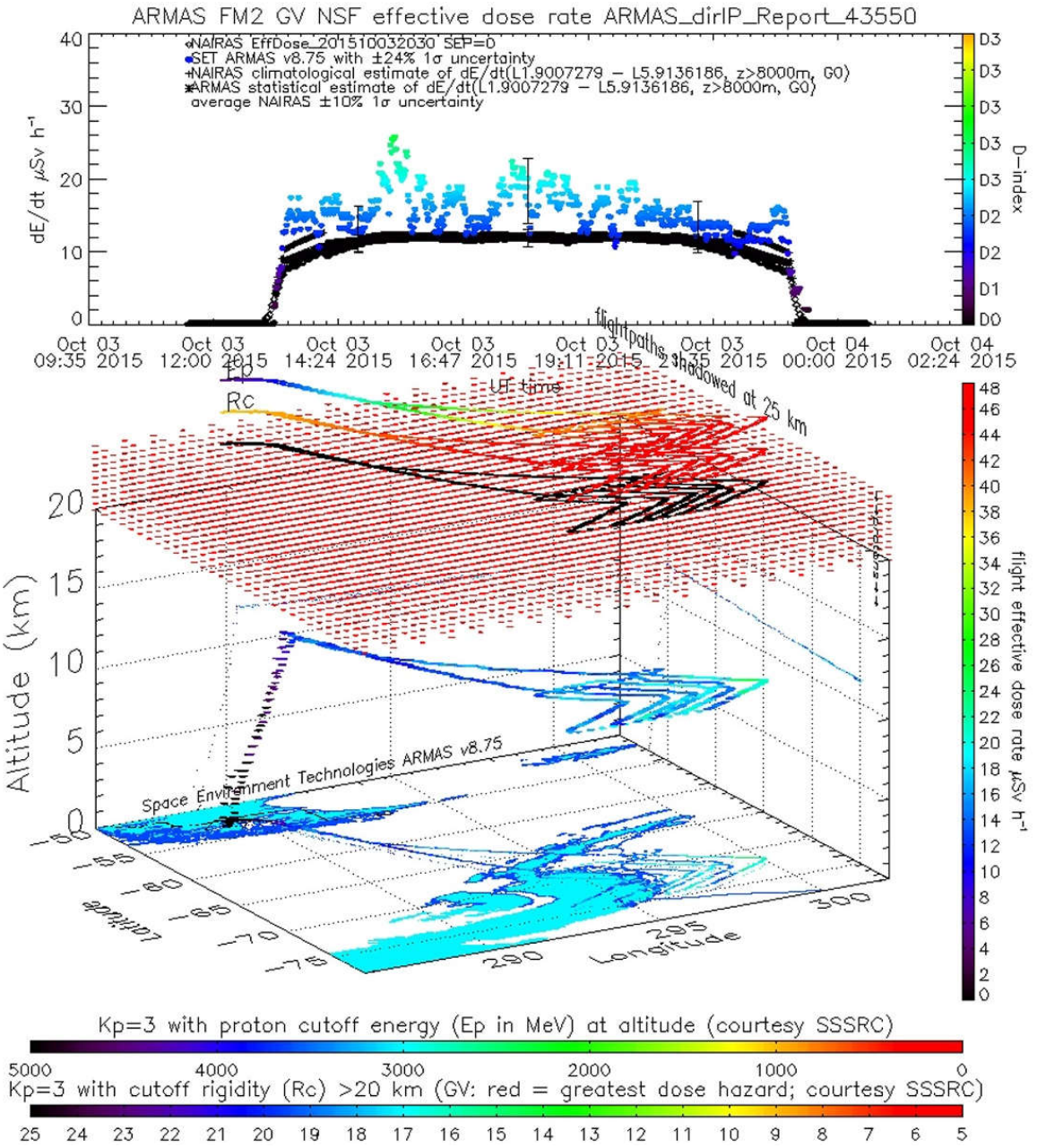

FIG. 5

Effective dose rates calculated as $\dot{E}$ from ARMAS (Tobiska et al., 2016).

quantity with the degree of impact. Furthermore, an index should communicate the relative severity of impacts and consequences of a particular space weather event to a nonexpert. NOAA introduced the Space Weather Scales, that is the G-Index for geomagnetic storms, the S-Index for solar radiation storms, and the R-Index for radio blackouts in 1999 (Poppe, 2000; Poppe & Jorden, 2006). However, while these indices have proven useful for effects on power systems, radio communications,

GPS-based transportation, and geosynchronous (GEO) satellite single-event effects (SEEs), they are not applicable to the radiation environment at aviation altitudes.

An example of this inadequacy is for the well-known Halloween storms on aviation on Oct. 29, 2003, when several airlines reacted to information of an ongoing severe solar radiation storm with a level of S4 on the NOAA S-scale. As a consequence of this alert, some flights from the United States to Europe flew at lower altitudes because those airlines had established a radiation storm action level at a threshold of S3 (Lieber, 2003; U.S. DoC, 2004). A detailed analysis later showed that the response was generally ineffective in terms of mitigating radiation exposure on the corresponding flights (Meier & Matthiä, 2014). These mitigation measures resulted in higher flight costs in fuel consumption and time as well as contributed to additional atmospheric pollution.

Why is the NOAA S-scale not useful for aviation radiation alerts? It is based on the >10 MeV integral proton flux, which is detected by GOES in geosynchronous orbit, that is, outside the Earth's atmosphere. According to the S-scale, an extreme solar radiation storm is defined by particle fluxes above 10^5 proton flux units (pfu), that is, protons $cm^{-2}\ s^{-1}\ sr^{-1}$. It provides useful information for the prompt assessment of radiation impacts in the GEO space environment for the operation of satellites and manned spaceflight.

At aviation altitudes the situation is different from the GEO environment. The Earth's magnetosphere and atmosphere play important roles in modifying the radiation field as described above. Model calculations have shown that the threshold for primary cosmic particles to overcome the atmospheric shielding and contribute to the aviation radiation field at mid- to low-latitudes is about 600 MeV. The vast majority of the impinging particles during the Halloween storms had energies below this threshold (Matthiä et al., 2014). As a result, the radiation intensity in most of the atmosphere was only slightly increased. Direct measurements at aviation altitudes (Beck et al., 2005) showed an increase in dose rates of about 30%;the University of Oulu (Finland) neutron monitor measured a count rate variation of about 5% at sea level during the peak of the associated GLE 65. This event demonstrated the shielding capability of the magnetosphere and atmosphere, which reduced the increase in the primary flux of >10 MeV protons by about five orders of magnitude as observed onboard GOES. Oulu, at sea level, observed an increase of only about 5% resulting in only moderate dose rate increases at aviation altitudes. A subsequent Forbush decrease in the GCRs then reduced the atmospheric radiation intensity for several days (Meier & Matthiä, 2014).

The comparatively low radiation exposure at aviation altitudes during the Halloween storms was not represented by the S-index, but it did raise the awareness of the need for a relevant aviation industry index. The concept of the Dose index (D-index) was developed to provide warnings of elevated radiation levels. It is based on the radiation exposure, such as from solar particles, added to the background GCR levels and is formed from the effective dose rate $\dot{E}_{sol}$, which can be derived from either measurements or model calculations.

The D-index covers a wide range of radiation exposure at aviation altitudes using small natural numbers in a base 2 calculation using effective dose rates ($\mu Sv\ h^{-1}$). It is defined as the smallest natural number, including zero, to satisfy the inequality:

$$\dot{E}_{sol} < 5\frac{\mu Sv}{h}2^{D} \tag{1}$$

The indices from D0 to D8, their corresponding ranges of effective dose rates, and their comparison with other natural radiation sources are listed in Table 1. Quiet space weather for aviation is characterized by D0-, D1-, or D2-levels. The D3-level, where there is an additional dose rate of >20 $\mu Sv\ h^{-1}$, indicates an

Table 1 D Index Definitions and Comparisons With Other Exposure Scenarios

D Index	Dose Rate Interval ($\mu Sv\ h^{-1}$)	Exposure is Comparable With
D0	$\dot{E}_{sol} < 5$	Variation of the natural background at cruising altitudes
D1	$5 \leq \dot{E}_{sol} < 10$	Natural background at high latitudes up to FL400
D2	$10 \leq \dot{E}_{sol} < 20$	Natural background at high latitudes between FL400 and FL600
D3	$20 \leq \dot{E}_{sol} < 40$	Average dose rate inside the International Space Station (ISS)
D4	$40 \leq \dot{E}_{sol} < 80$	Average dose rate during extravehicular activity (EVA) on the ISS
D5	$80 \leq \dot{E}_{sol} < 160$	Dose of a north Atlantic return flight received or approximately one chest X-ray per hour
D6	$160 \leq \dot{E}_{sol} < 320$	Daily dose at aviation altitudes and high latitudes received in 1 h
D7	$320 \leq \dot{E}_{sol} < 640$	Daily average dose inside the ISS received in 1 h
D8	$640 \leq \dot{E}_{sol} < 1280$	Three-month dose for living on ground in most countries received in 1 h

elevated radiation intensity that can be used by air traffic management to trigger a radiation alert. The D-index can be used within the framework of already existing warning systems (Fig. 5, top panel). For example, this scale has already been used by the Federal Aviation Administration's (FAA) Solar Radiation Alert System (ESRAS); an alert is issued if D3 is exceeded at any altitude between 30,000 and 70,000 ft for each of three consecutive 5-min periods (Copeland et al., 2009; Copeland, 2016). The dose rate for triggering a D3 alert corresponds roughly to the average dose rate inside the International Space Station (ISS) that many astronauts and cosmonauts are exposed to for several months from GCR and trapped radiation. It is worth mentioning that the dose rates inside the ISS will generally be much higher during such a solar particle event due to the absence of atmospheric shielding. The D-index has also been used to provide space weather-induced radiation dose rate information for several European airlines since 2014.

An important feature of the D-index is its application within a particular volume cell of the atmosphere (latitude, longitude, altitude). In this context, it can be used to communicate a differentiated picture about the radiation field above specific geographic regions and at unique altitudes. This is similar to the communication of terrestrial weather parameters such as winds, temperature, air pressure, and humidity. For example, the increased radiation exposure for a particular region can be generalized for commercial aviation and a local warning index, D_L, can be derived from the maximum regional dose rate at a flight level of 41,000 ft (FL410). This would characterize the upper airspace as the worst-case scenario. Furthermore, the provision of individual indices for particular flights, as D_F-values, is possible as well.

6 EXAMPLE OF AN EXTREME EVENT

Although there have been no warning situations since the development of the D-index, as of May 2017 the application of the D-index can be demonstrated with GLE 70, which took place on Dec. 13, 2006. GLE 70 is an excellent example illustrating the D-index concept. This event showed a sharply peaked time profile and a spatial distribution leading to relatively large intensity increases at eastern latitudes

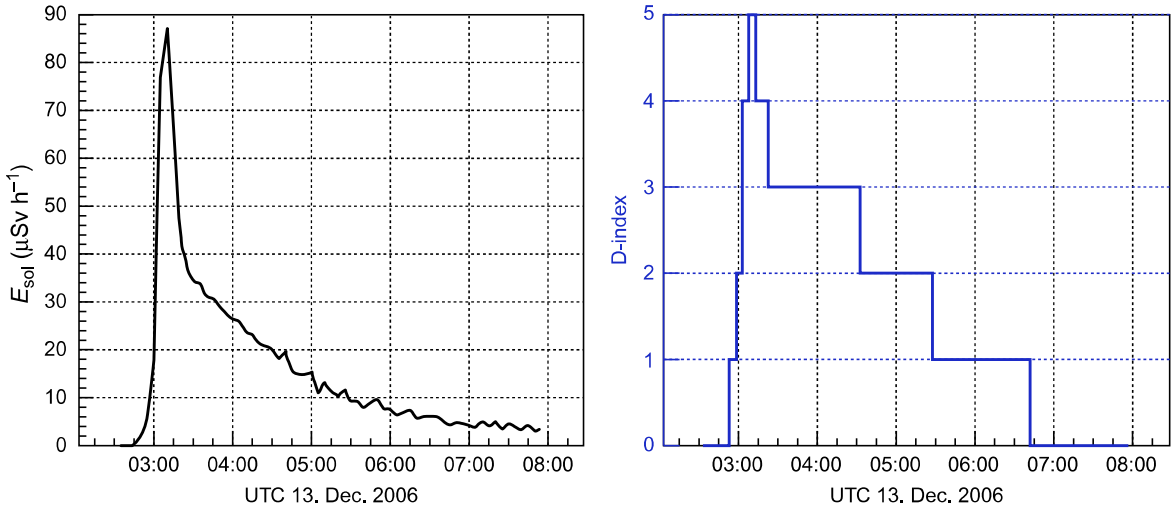

FIG. 6

Effective doses and corresponding D-indices at an altitude of 41,000 ft during GLE 70, a large solar proton event that occurred Dec. 13, 2006, as calculated by PANDOCA (Matthiä et al., 2014).

in Russia and Europe in the initial phase of the event (Fig. 6). In the later isotropic phase of the event a weaker response in cosmic ray intensities was recorded in North America.

The GLE was related to an X3 solar flare on the NOAA scale when it originated in the solar western hemisphere (5S23W) at 2:39 UTC. Neutron monitor stations in Europe, such as Kiel and Oulu, recorded count rate increases starting between 2:50 and 2:55 UTC marking the onset of GLE ~15 min after the peak in the X-ray flux. Maximum intensities were measured at 3:05 UTC. Stations in North America, such as Inuvik and Calgary, recorded the beginning of the event about 10 min later. Much weaker peak increases were measured by these stations about half an hour later between 3:30 and 3:40 UTC. Matthiä et al. (2009) performed a detailed analysis of this event using data from the complete neutron monitor network.

The left column of Fig. 7 illustrates the global distribution of dose rates at 41,000 ft when maximum values were reached (3:10 UTC) and about half an hour later (3:35 UTC) as calculated by the PANDOCA model (Matthiä et al., 2014). On the right of Fig. 7 are the corresponding D-indices. In the initial phase of the eventmostly eastern latitudes were affected as shown in the neutron monitor stations' measurements. Peak dose rates were calculated to be ~80–90 μSv h^{-1} corresponding to a D-index of 5 (Fig. 6). However, these relatively large values only occurred regionally. The Americas were minimally affected at that time. While the global D-index for the event was 5, a regionally derived index for North America would have been 0. About half an hour later at 3:35 UTC, however, the impact of the event on the radiation exposure at aviation altitudes was not limited to specific regions anymore and only showed a typical pattern of magnetic shielding (lower row of Fig. 7). At that time the maximum dose rate had decreased to about 30–40 μSv h^{-1} (D3), but previously unaffected regions showed an increase in exposure as well. All areas above 60°N and below 60°S were ultimately affected with a D-index of 2 or 3.

Matthiä et al. (2015) investigated the effectiveness of mitigation measures and their economic impacts related to delay and fuel consumption for a transatlantic flight during GLE 70. If the increase

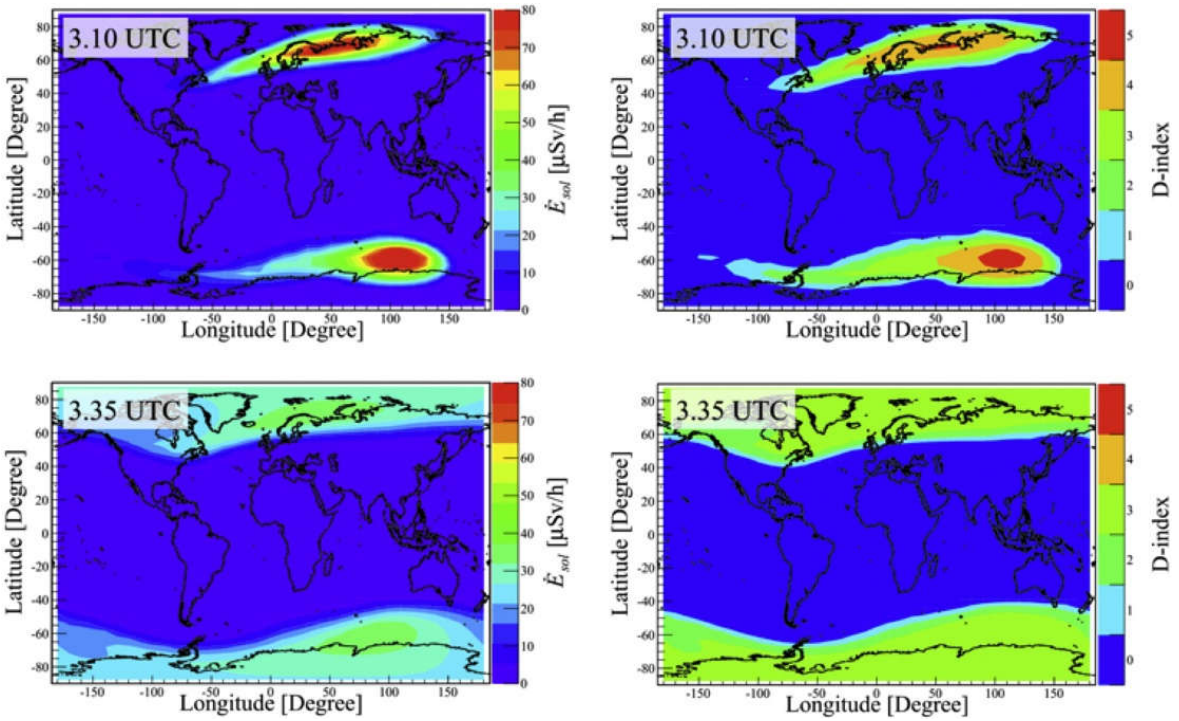

FIG. 7

Global distribution of effective dose rates and D-indices at an altitude of 41,000 ft during GLE 70, as calculated using PANDOCA.

in dose rate as expressed by the D-index could be communicated to the cockpit, then an appropriate action might be taken. The communication could typically be done through ACARS (Aircraft Communications Addressing and Reporting System). In Matthiä et al. (2015) the response to the event was (i) lower the flight altitude after the increase of the dose rates, (ii) adapt the flight velocity, and (iii) return to nominal flight altitudes after the additional dose rates had dropped below a threshold.

It was shown that in the ideal case, that is a prompt response to an increase in the radiation exposure caused by this GLE, the total effective dose on the flight could have been reduced up to 42% by lowering the flight altitude and using the contingency aircraft fuel (i.e., an additional fuel consumption of up to 5%). If the aircraft had returned to the most economical flight altitude after the dose rate had dropped below 10 μSv h^{-1} (D-index of 1 or 0), the total effective dose reduction would have been about 30%. For the ideal scenario this return to the original flight altitude occurred at 5:18 UTC. After this time the radiation exposure was at the GCR background or below. By comparison, the integral proton flux measured by GOES had not even reached its maximum at that time. The integral flux >10 MeV, which is the basis for the NOAA S-scale, reached its maximum not before 10:30 UTC. At that time, the event was essentially over in terms of radiation exposure at aviation altitudes. This example demonstrates that an ideal response to an event could be based on dose rates at aviation altitudes and could have been supported using the D-index. For the calculated flight, the D-index would have remained at D1 rather than D3 in case of no response.

7 CONCLUSION

The intensity of the radiation field due to cosmic radiation at aviation altitudes during quiet space weather conditions is, in terms of effective dose rate, $\dot{E}$, more than one order of magnitude higher than the average radiation environment from all natural sources on the ground in most countries. As a consequence, aircrew and frequent flyers are exposed to higher levels of ionizing radiation than the average population. This has led to legal regulations and the implementation of corresponding radiation protection measures in many countries, including in the European Union, Switzerland, and South Korea. In the United States, guidelines have been issued; the FAA funds research, provides software, operates a Solar Radiation Alert system, and maintains an issue-related website at http://www.faa.gov/data_research/research/med_humanfacs/aeromedical/radiobiology/ (Freidberg et al., 1999; Friedberg & Copeland, 2011).

Extreme space weather events are still not monitored during flight in real time and GLEs have often been used as a surrogate for extreme solar cosmic ray particle events. Their occurrence can bring about a further, albeit short-term, significant increase in radiation exposure, although not all GLEs have the same energy spectrum. The actual additional total exposure at cruising altitudes during *short-term* events is likely to be moderate in comparison to the ordinary *annual* radiation exposure from other natural and artificial sources, even though these events do present unknown consequences for an individual's health. Further research leading to effective and efficient real-time monitoring is necessary to better understand the effects of the aviation radiation environment.

An index for the assessment of the radiation field at aviation altitudes during extreme space weather events has merit and is discussed. Any index requires a close connection between an observable physical quantity and the degree of an impact. This is the basis of the D-index that is derived from the effective dose rate using either measurements or models. The effective dose rate, $\dot{E}$, is the fundamental physical quantity used for characterizing radiation fields in radiation protection practices. The D-index is a decision-aid tool that can provide timely and useful information to the aviation community about space weather effects related to radiation at aviation altitudes. The D-index is flexible in its global or regional application and is independent of the radiation model or measurement used for its assessment. In this respect, it also supports national level regional warning centers (RWCs), which have been successfully used in the field of terrestrial weather for many years. The responsible authorities for different countries or regions can select baseline measurements or models in consideration of their own needs. The feasibility of mitigating measures for aviation altitude radiation during a space weather event was described with the example of a study using GLE 70. Timely space weather information based on the D-index might have reduced the radiation exposure of crew and passengers during this event from D3 to D1, thus improving aviation crew and passenger health and safety.

ACKNOWLEDGMENTS

The authors thank the reviewers for their timely and insightful comments that have improved this paper. The authors acknowledge the financial support for ARMAS from the original NASA NAIRAS project contract NNL07AA00C, the NASA SBIR Phase I and Phase II program contracts NNX11CH03P and NNX12CA78C, the NASA AFRC Phase III contracts NND14SA64P and NND15SA55C, and the South Korean Space Weather

Center matching funds for SBIR Phase IIE. Gracious flight support for ARMAS instruments has been provided by the NASA Airborne Sciences Program and Armstrong Flight Research Center. The NOAA Space Weather Prediction Center facilitated use of the NOAA Gulfstream IV through their good offices as did the National Center for Atmospheric Research High Altitude Observatory for the use of the National Science Foundation Gulfstream V. In accordance with the AGU data policy, the ARMAS archival data used in this paper, as well as from all flights, is publically available from the ARMAS website at http://sol.spacenvironment.net/armas_ops/Archive/. Other support for this work was provided by the German Aerospace Center (DLR) and the Aerospace Medical Research Division of the FAA Civil Aerospace Medical Institute.

REFERENCES

Al Anid, H., Lewis, B.J., Bennett, L.G.I., Takada, M., 2009. Modelling of radiation exposure at high altitudes during solar storms. Radiat. Prot. Dosim. 136 (4), 311–316. https://doi.org/10.1093/rpd/ncp127.

Andriopoulou, M., Mavromichalaki, H., Preka-Papadema, P., Plainaki, C., Belov, A., Eroshenko, E., 2011. Solar activity and the associated ground level enhancements of solar cosmic rays during solar cycle 23. Astrophys. Space Sci. Trans. 7, 439–443.

Atwell, W., Tylka, A.J., Dietrich, W.F., Rojdev, K., Matzkind, C., 2016. Probability estimates of solar proton doses during periods of low sunspot number for short duration missions. In: 46th International Conference on Environmental Systems, ICES-2016-453, 10-14 July 2016, Vienna, Austria.

Beck, P., Ambrosi, P., Schrewe, U., O'Brien, K., 1999. ACREM, aircrew radiation exposure monitoring, Final report of European Commission contract F14P-CT960047, OEFZS, Rep. G-0008.

Beck, P., Latocha, M., Rollet, S., Stehno, G., 2005. TEPC reference measurements at aircraft altitudes during a solar storm. Adv. Space Res. 36 (9), 1627–1633.

Beck, P., Dyer, C., Fuller, N., Hands, A., Latocha, M., Rollet, S., Spurny, F., 2009. Overview of on-board measurements during solar storm periods. Radiat. Prot. Dosim. 136 (4), 297–303. https://doi.org/10.1093/rpd/ncp208.

Carmichael, H., 1964. Cosmic rays. In: IQSY Instruction Manual No. 7. IQSY Secretariat, London.

Copeland, K., 2016. ESRAS: an enhanced solar radiation alert system. Federal Aviation Administration, Civil Aerospace Medical Institute, Oklahoma City, OK. DOT Report No. DOT/FAA/AM-16/5.

Copeland, K., 2017. CARI-7A: development and validation. Radiat. Prot. Dosim. https://doi.org/10.1093/rpd/ncw369.

Copeland, K., Sauer, H.H., Duke, F.E., Friedberg, W., 2008. Cosmic radiation exposure of aircraft occupants on simulated high-latitude flights during solar proton events from 1 January 1986 through 1 January 2008. Adv. Space Res. 42, 1008–1029. https://doi.org/10.1016/j.asr.2008.03.001.

Copeland, K., Sauer, H., Friedberg, W., 2009. Solar radiation alert system. Federal Aviation Administration, Civil Aerospace Medical Institute, Oklahoma City, OK. DOT Report No. DOT/FAA/AM-09/6 (revised 30 May 2008).

Dyer, C., Lei, F., 2001. Monte-Carlo calculations of the influence on aircraft radiation environments of structures and solar particle events. IEEE Trans. Nucl. Sci. 48 (6), 1987–1995.

Dyer, C.S., Truscott, P., 1999. Cosmic radiation effects on avionics. Radiat. Prot. Dosim. 86 (4), 337–342.

Dyer, C.S., Sims, A.J., Farren, J., Stephen, J., 1990. Measurements of solar flare enhancements to the single event upset environment in the upper atmosphere. IEEE Trans. Nucl. Sci. 37, 1929–1937. https://doi.org/10.1109/23.101211.

Dyer, C.S., Lei, F., Clucas, S.N., Smart, D.F., Shea, M.A., 2003. Solar particle enhancements of single event effect rates at aircraft altitudes. IEEE Trans. Nucl. Sci. 50 (6), 2038–2045.

Dyer, C., Hands, A., Fan, L., Truscott, P., Ryden, K.A., Morris, P., Getley, I., Bennett, L., Bennett, B., Lewis, B., 2009. Advances in measuring and modeling the atmospheric radiation environment. IEEE Trans. Nucl. Sci. 6 (1), 3415–3422.

ECRP (European Commission Radiation Protection) 140, 2004. Cosmic Radiation Exposure of Aircraft Crew, Compilation of Measured and Calculated Data, European communities.

Felsberger, E., O'Brien, K., Kindl, P., 2009. IASON-FREE: theory and experimental comparisons. Radiat. Prot. Dosim. 136 (4), 267–273. https://doi.org/10.1093/rpd/ncp128.

Freidberg, W., Copeland, K., Duke, F.E., O'Brien, K., Darden, E.B., 1999. Guidelines and technical information provided by the U.S. Federal Aviation Administration to promote radiation safety for air carrier crew members. Radiat. Prot. Dosim 86, 323.

Friedberg, W., Copeland, K., 2003. What aircrews should know about their occupational exposure to ionizing radiation ionizing. Federal Aviation Administration, Civil Aerospace Medical Institute, Oklahoma City, OK. DOT Report No. DOT/FAA/AM-03/16.

Friedberg, W., Copeland, K., 2011. Ionizing radiation in earth's atmosphere and in space near earth. Federal Aviation Administration, Civil Aerospace Medical Institute, Oklahoma City, OK. DOT Report No. DOT/FAA/AM-11/9.

Gerontidou, M., Vassilaki, A., Mavromichalaki, H., Kurt, V., 2002. Frequency distributions of solar proton events. J. Atmos. Sol.-Terr. Phys. 64, 489–496.

Gersey, B., Wilkins, R., Atwell, W., Tobiska, W.K., Mertens, C., 2012. Tissue equivalent proportional counter microdosimetry measurements aboard high-altitude and commercial aircraft. AIAA 2012–3636In: AIAA 42nd International Conference on Environmental Systems, San Diego, California, 15–19 July.

Getley, I.L., Duldig, M.L., Smart, D.F., Shea, M.A., 2005. Radiation dose along North American transcontinental flight paths during quiescent and disturbed geomagnetic conditions. Space Weather 3. https://doi.org/10.1029/2004SW000110 S01004.

Hands, A., Dyer, C.S., 2009. A technique for measuring dose equivalent and neutron fluxes in radiation environments using silicon diodes. IEEE Trans. Nucl. Sci. 56 (1), 3442–3449.

Hatton, C.J., 1971. The neutron monitor. In: Progress in Elementary Particle and Cosmic Ray Physics, vol. 10. pp. 3–102.

Hwang, J., Dokgo, K., Choi, E., Kin, K.-C., Kim, H.-P., Cho, K.-S., 2014. Korean Radiation Exposure Assessment Model for aviation route dose. In: KREAM, KSS Fall meeting, Jeju, Korea, October 29-31.

IARC (International Agency for Research on Cancer), 2000. Ionizing radiation, Part 1, X- and γ-radiation and neutrons. In: IARC Monographs on the Evaluation of Carcinogenic Risks to Humans. vol. 75. IARC Press, Lyon, France. ISBN: 92 832 1275 4.

ICRP 2007, 2007. Recommendations of the ICRP, ICRP Pub. 103. Ann. ICRP 37 (2-4), 1–332.

Iles, R.H.A., Jones, J.B.L., Taylor, G.C., Blake, J.B., Bentley, R.D., Hunter, R., Harra, L.K., Coates, A.J., 2004. Effect of solar energetic particle (SEP) events on the radiation exposure levels to aircraft passengers and crew: case study of 14 July 2000 SEP event. J. Geophys. Res. 109. https://doi.org/10.1029/2003JA010343 A11103.

Johnston, C.O., 2008. A Comparison of EAST Shock-Tube Radiation Measurements With a New Radiation Model. AIAA Paper 2008-1245.

Joyce, C.J., Schwadron, N.A., Wilson, J.K., Spence, H.E., Kasper, J.C., Golightly, M., Blake, J.B., Townsend, L.W., Case, A.W., Semones, E., Smith, S., Zeitlin, C.J., 2014. Radiation modeling in the Earth and Mars atmospheres using LRO/CRaTER with the EMMREM Module. Space Weather 12, 112–119. https://doi.org/10.1002/2013SW000997.

Kyllönen, J.E., Lindborg, L., Samuelson, G., 2001. Cosmic radiation measurements on board aircraft with the variance method. Radiat. Prot. Dosim. 93, 197–205.

Latocha, M., Autischer, M., Beck, P., Bottolier–Depois, J.F., Rollet, S., Trompier, F., 2007. The results of cosmic radiation in-flight TEPC measurements during the CAATER flight campaign and comparison with simulation. Radiat. Prot. Dosim. 125 (1–4), 412–415. https://doi.org/10.1093/rpd/ncl123.

Latocha, M., Beck, P., Rollet, S., 2009. AVIDOS—a software package for European accredited aviation dosimetry. Radiat. Prot. Dosim. 136 (4), 286. https://doi.org/10.1093/rpd/ncp126.

Latocha, M., Beck, P., Bütikofer, P., Thommesen, H., 2014. AVIDOS 2.0—Current Developments for the Assessment of Radiation Exposure at Aircraft Altitudes Caused by Solar Cosmic Radiation Exposure, European Space Weather Week, Liege, 17-21 November. http://stce.be/esww11.

Lee, J., Nam, U.-W., Pyo, J., Kim, S., Kwon, Y.-J., Lee, J., Park, I., Kim, M.-H.Y., Dachev, T.P., 2015. Short-term variation of cosmic radiation measured by aircraft under constant flight conditions. Space Weather 13, 797–806. https://doi.org/10.1002/2015SW001288.

Lieber, R., 2003. Solar storm rekindles concern over whether radiation hurts fliers. Wall Street J. 30th October, http://online.wsj.com/news/articles/SB106744850896766200.

Mares, V., Maczka, T., Leuthold, G., Ruhm, M., 2009. Air crew dosimetry with a new version of EPCARD. Radiat. Prot. Dosim. 136 (4), 262–266. https://doi.org/10.1093/rpd/ncp129.

Matthiä, D., Heber, B., Reitz, G., Sihver, L., Berger, T., Meier, M., 2009. The ground level event 70 on December 13th, 2006 and related effective doses at aviation altitudes. Radiat. Prot. Dosim. 136 (4), 304–310. https://doi.org/10.1093/Rpd/Ncp141.

Matthiä, D., Meier, M.M., Reitz, G., 2014. Numerical calculation of the radiation exposure from galactic cosmic rays at aviation altitudes with the PANDOCA core model. Space Weather 12, 161. https://doi.org/10.1002/2013SW001022.

Matthiä, D., Schaefer, M., Meier, M.M., 2015. Economic impact and effectiveness of radiation protection measures in aviation during a ground level enhancement. J. Space Weather Space Clim. 5, A17. https://doi.org/10.1051/swsc/2015014.

McCall, M.J., Lemay, F., Bean, M.R., Lewis, B.J., Bennett, L.G., 2009. Development of a pre-dictive code for aircrew radiation exposure. Radiat. Prot. Dosim. 136 (4), 274–281. https://doi.org/10.1093/rpd/ncp130.

McCracken, K.G., Moraal, H., Shea, M.A., 2012. The high-energy impulsive ground-level enhancement. Astrophys. J. 761, 101 2012 December 20.

Meier, M.M., Matthiä, D.D., 2014. A space weather index for the radiation field at aviation altitudes. J. Space Weather Space Clim. 4, A13.

Meier, M.M., Hubiak, M., Matthiä, D., Wirtz, M., Reitz, G., 2009. Dosimetry at aviation altitudes (2006–2008). Radiat. Prot. Dosim. 136 (4), 251–255.

Meier, M.M., Trompier, F., Ambrozova, I., Kubancak, J., Matthiä, D., Ploc, O., Santen, N., Wirtz, M., 2016a. CONCORD: comparison of cosmic radiation detectors in the radiation field at aviation altitudes. J. Space Weather Space Clim. 6, A24. https://doi.org/10.1051/swsc/2016017.

Meier, M.M., Matthiä, D., Forkert, T., Wirtz, M., Scheibinger, M., Hübel, R., Mertens, C.J., 2016b. RaD-X: complementary measurements of dose rates at aviation altitudes. Space Weather 14. https://doi.org/10.1002/2016SW001418.

Mertens, C.J., Kress, B.T., Wiltberger, M., Tobiska, W.K., Grajewski, B., Xu, X., 2012. Atmospheric ionizing radiation from galactic and solar cosmic rays. In: Nenoi, M. (Ed.), Current Topics in Ionizing Radiation Research. InTech.

Mertens, C.J., Meier, M.M., Brown, S., Norman, R.B., Xu, X., 2013. NAIRAS aircraft radiation model development, dose climatology, and initial validation. Space Weather 11, 603. https://doi.org/10.1002/swe.20100.

Mertens, C.J., Gronoff, G.P., Norman, R.B., Hayes, B.M., Lusby, T.C., Straume, T., Tobiska, W.K., Hands, A., Ryden, K., Benton, E., Wiley, S., Gersey, B., Wilkins, R., Xu, X., 2016. Cosmic radiation dose measurements from the RaD-X flight campaign. Space Weather 14. https://doi.org/10.1002/2016SW001407.

Mishev, A.L., Adibpour, F., Usoskin, I.G., Felsberger, E., 2015. Computation of dose rate at flight altitudes during ground level enhancements no. 69, 70 and 71. Adv. Space Res. 55, 354–362.

Mutuel, L.H., 2016. Single Event Effects Mitigation Techniques Report, Department of Transportation/Federal Aviation Administration, TC-15/62, February 2016.

Normand, E., Oberg, D.L., Wert, J.L., Ness, J.D., Majewski, P.P., Wender, S., Gavron, A., 1994. Single event upset and charge collection measurements using high energy protons and neutrons. IEEE Trans. Nucl. Sci. 41 (6), 2203–2209.

Normand, E., Vranish, K., Sheets, A., Stitt, M., Kim, R., 2006. Quantifying the double-sided neutron SEU threat, from low energy (thermal) and high energy (>10 MeV) neutrons. IEEE Trans. Nucl. Sci. 53 (6), 3587–3595.

O'Brien, K., Sauer, H.H., 2000. An adjoint method of calculations of solar-particle-event dose rates. Technology 7 (2-4), 449–456.

O'Brien, K., Friedberg, W., Sauer, H.H., Smart, D.F., 1996. Atmospheric cosmic rays and solar energetic particles at aircraft altitudes. Environ. Int. 22 (Suppl. 1), S9–S44.

Ploc, O., Ambrozova, I., Kubancak, J., Kovar, I., Dachev, T.P., 2013. Publicly available database of measurements with the silicon spectrometer Liulin onboard aircraft. Radiat. Meas. 58, 107–112.

Poppe, B., 2000. New scales help public, technicians understand space weather. Eos Trans. Am. Geophys. Union 81 (29), 322–328.

Poppe, B., Jorden, K., 2006. Sentinels of the Sun. Johnson Books, Boulder, CO. ISBN 1-55566-379-6.

Regener, E., Pfotzer, G., 1935. Vertical intensity of cosmic rays by threefold coincidences in the stratosphere. Nature 136, 718.

Sato, T., 2015. Analytical model for estimating terrestrial cosmic ray fluxes nearly anytime and anywhere in the world: extension of PARMA/EXPACS. PLoS One. 10 (12), e0144679.

Sato, T., Yasuda, H., Niita, K., Endo, A., Sihver, L., 2008. Development of PARMAPHITS-based analytical radiation model in the atmosphere. Radiat. Res. 170, 244.

Schwadron, N.A., Baker, T., Blake, B., Case, A.W., Cooper, J.F., Golightly, M., Jordan, A., Joyce, C., Kasper, J., Kozarev, K., Mislinski, J., Mazur, J., Posner, A., Rother, O., Smith, S., Spence, H.E., Townsend, L.W., Wilson, J., Zeitlin, C., 2012. Lunar radiation environment and space weathering from the Cosmic Ray Telescope for the Effects of Radiation (CRaTER). J. Geophys. Res. Planets 117. https://doi.org/10.1029/2011JE003978. E00H13.

Shea, M.A., Smart, D.F., 2012. Space weather and the ground-level solar proton events of the 23rd solar cycle. Space Sci. Rev. 171, 161–188.

Simpson, J.A., 1983. Elemental and isotopic composition of the galactic cosmic rays. Annu. Rev. Nucl. Part. Sci. 33, 323–382. https://doi.org/10.1146/annurev.ns.33.120183.001543.

Simpson, J.A., 2000. The cosmic ray nucleonic component: the invention and scientific uses of the neutron monitor—(Keynote lecture). Space Sci. Rev. 93, 11–32. https://doi.org/10.1023/A:1026567706183.

Singleterry, R.C., Blattnig, S.R., Clowdsley, M.S., Qualls, G.D., Sandridge, C.A., Simonsen, L.C., Norbury, J.W., Slaba, T.C., Walker, S.A., Badavi, F.F., Spangler, J.L., Aumann, A.R., Zapp, E.N., Rutledge, R.D., Lee, K.T., Norman, R.B., 2010. OLTARIS: On-Line Tool for the Assessment of Radiation in Space, NASA/TP–2010-216722. NASA Langley Research Center, Hampton, Virginia.

Spence, H.E., Case, A., Golightly, M.J., Heine, T., Larsen, B.A., Blake, J.B., Caranza, P., Crain, W.R., George, J., Lalic, M., Lin, A., Looper, M.D., Mazur, J.E., Salvaggio, D., Kasper, J.C., Stubbs, T.J., Doucette, M., Ford, P., Foster, R., Goeke, R., Gordon, D., Klatt, B., O'connor, J., Smith, M., Onsager, T., Zeitlin, C., Townsend, L., Charara, Y., 2010. CRaTER: The Cosmic Ray Telescope for the Effects of Radiation Experiment on the Lunar Reconnaissance Orbiter Mission. Space Sci. Rev. 150 (1-4), 243–284.

Tobiska, W.K., Gersey, B., Wilkins, R., Mertens, C., Atwell, W., Bailey, J., 2014a. U.S. Government shutdown degrades aviation radiation monitoring during solar radiation storm. Space Weather 12. https://doi.org/10.1002/2013SW001015.

Tobiska, W.K., Gersey, B., Wilkins, R., Mertens, C., Atwell, W., Bailey, J., 2014b. Reply to comment by Rainer Facius et al. on "U.S. Government shutdown degrades aviation radiation monitoring during solar radiation storm," Space Weather 12, 320–321. https://doi.org/10.1002/2014SW001074.

Tobiska, W.K., Atwell, W., Beck, P., Benton, E., Copeland, K., Dyer, C., Gersey, B., Getley, I., Hands, A., Holland, M., Hong, S., Hwang, J., Jones, B., Malone, K., Meier, M.M., Mertens, C., Phillips, T., Ryden, K., Schwadron, N., Wender, S.A., Wilkins, R., Xapsos, M.A., 2015. Advances in atmospheric radiation

measurements and modeling needed to improve air safety. Space Weather 13, 202–210. https://doi.org/10.1002/2015SW001169.

Tobiska, W.K., Bouwer, D., Smart, D., Shea, M., Bailey, J., Didkovsky, L., Judge, K., Garrett, H., Atwell, W., Gersey, B., Wilkins, R., Rice, D., Schunk, R., Bell, D., Mertens, C., Xu, X., Wiltberger, M., Wiley, S., Teets, E., Jones, B., Hong, S., Yoon, K., 2016. Global real-time dose measurements using the Automated Radiation Measurements for Aerospace Safety (ARMAS) system. Space Weather 14, 1053–1080.

U.S. DOC (Department of Commerce), 2004. Service Assessment—Intense Space Weather Storms October 19–November 07, 2003, 17-18. Available from http://www.swpc.noaa.gov/Services/SWstorms_assessment.pdf.

UNSCEAR (United Nations Scientific Committee on the Effect of Atomic Radiation)., 2000. Sources and effect of ionizing radiation, United Nations Scientific Committee on the Effect of Atomic Radiation UNSCEAR 2000 Report to the General Assembly, with Scientific Annexes, vol. II, Annex G.

Wissmann, F., Reginatto, M., Möller, T., 2010. Ambient dose equivalent at flight altitudes: a fit to a large set of data using a Bayesian approach. J. Radiol. Prot. 30, 513–524.